Fabrication and characterization of a negative-refractive-index composite metamaterial

A. F. Starr,* P. M. Rye, D. R. Smith,[†] and S. Nemat-Nasser

Department of Mechanical and Aerospace Engineering, University of California, San Diego, La Jolla, California 92093, USA
(Received 21 March 2004; published 17 September 2004)

We have designed, produced, and experimentally characterized 2.7 mm thick composite panels having negative refractive index between 8.4 and 9.2 GHz. The composite metamaterial is fabricated using conventional commercial multilayer circuit-board lithography; three-dimensional physical (as opposed to electromagnetic) structure is introduced by the use of vias to form sections of the scattering elements in the direction perpendicular to the circuit board surfaces. From scattering parameter measurements, we show that the complex permittivity, permeability, index, and impedance of the composite can be unambiguously determined. The measurements enable the quantitative determination of the negative index band and associated losses. The extracted material parameters are shown to be in excellent agreement with simulation results.

Negative refraction is a phenomenon only recently appreciated, but which has generated considerable interest because of its potential role in physical phenomena, applications, and devices. While there have now been many suggested paths toward the design of a material whose effective index-of-refraction is negative, a rigorous approach is to design a material whose electric permittivity (ε) and magnetic permeability (μ) are simultaneously negative. This approach to negative refraction was hypothesized by Veselago in 1968,[1] who described both the limitations of negative materials as well as the unique wave propagation characteristics such materials would possess.

While there are no known naturally occurring materials or compounds that exhibit simultaneously negative ε and μ, artificially structured materials can be designed whose effective ε and μ, as derived from effective medium arguments, are both negative over a finite frequency band.[2–4]

In 2001, a *metamaterial* medium was constructed and used to demonstrate experimentally negative refraction at microwave frequencies.[5] This material made use of an array of dual split-ring resonators (SRRs) that provided a negative μ, interspersed with an array of wires that provided a negative ε. Because the region of negative ε overlapped the region of negative μ associated with the SRRs, the composite had a frequency band of negative index. In this material, the SRRs and wires were patterned by optical lithography on either side of a circuit board substrate. Similar designs have been utilized in further experimental confirmations of negative refraction.[6,7]

The SRR/wire structures have proven useful in demonstrating the underlying wave propagation behavior of negative index materials; moreover, these structures have provided a basis for the further development of interesting metamaterials. However, the SRR elements impose a specific burden on fabrication that adds a layer of complexity to current negative index metamaterial designs. Unlike straight wires, the SRR elements typically require a significant length in the direction of wave propagation in order to provide a strong magnetic response. To meet this constraint, previous circuit-board based SRR designs have required sectioning a planar SRR circuit board into strips, or using sheets of the planar circuit boards, oriented so that the incident wave direction is in the plane and the SRR axes lie perpendicular to the propagation direction of the incident wave.

While the initial planar metamaterial designs may have limitations, these structures have shown the value of leveraging circuit board technology to develop artificial materials. In the present work, we utilize multilayer circuit board techniques to fabricate a negative index metamaterial structure (Fig. 1) that requires no additional assembly step. The design we present thus departs from the need for a "wine-crate" assembly step inherent to previous metamaterials, and is suited for mass production.

In the current design, single SRRs are used rather than dual SRRs to achieve negative μ. In the previous metamaterial structures, nested dual SRRs were utilized as a convenient means of increasing the capacitance of the resonator element; here, the combination of the diameter of the via pads and the higher dielectric constant of the intervening layer introduces sufficient capacitance such that the additional capacitance of the second ring is not necessary.
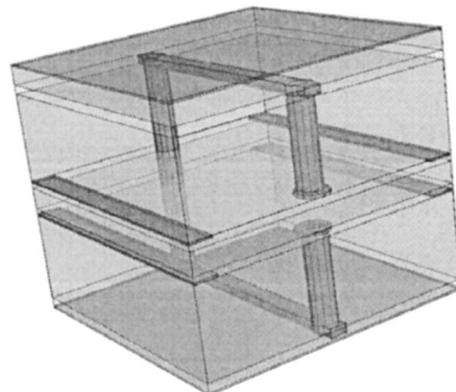

FIG. 1. A single unit cell of the negative index composite. The negative permeability is achieved by ring resonators, formed from copper strips on the upper and lower surfaces, connected by vias that run through the laminated structure. Blind vias (shown in the foreground) form a gap in the center to introduce capacitance. Copper strips are patterned on the central laminate, giving rise to the negative permittivity of the structure.

Cross-section of split ring element

0.032" Rogers 4003

2 x 0.0015" Gore Speedboard
+0.008" Rogers 4003
+ 2 x 0.0015" Gore Speedboard
(~0.014" total thickness)

Total thickness = 1.981 mm
= 0.078"

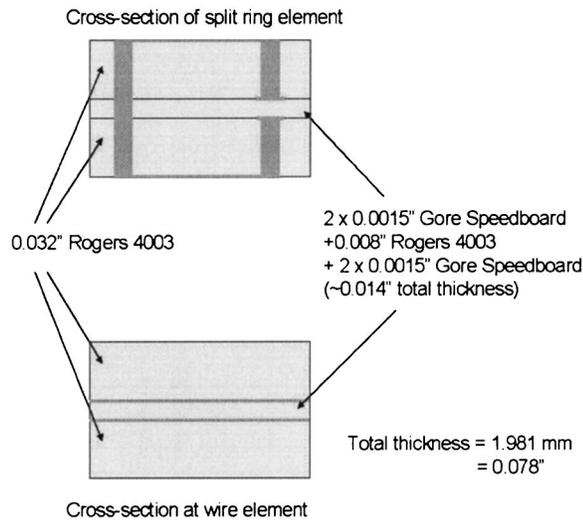Cross-section at wire element

FIG. 2. Detail of the original design of the single ring resonator (SRR).

The composite is assembled from three laminated layers. The top and bottom layers consist of Rogers 4003 circuit board laminates ($\varepsilon=3.38$, tan $\delta=0.003$), with a prepreg layer of Gore SpeedBoard ($\varepsilon=2.56$, tan $\delta=0.004$). The dimensions are indicated in the cross section shown in Fig. 2, as well as in Table I. The layers are bound together by a layer of adhesive at the interfaces between the Gore and Rogers circuit

TABLE I. Measured and simulated parameters of the negative index composite structure in millimeters.

Dimension	Measurement	Simulated
Unit cell		
X	3.01 ± 0.01	3.00
Y	3.01 ± 0.01	3.00
Z	2.62 ± 0.01	2.616
Through via		
Outer radius	0.131 ± 0.006	$0.130\ 5813$
Inner radius	0.090 ± 0.009	$0.089\ 6786$
Height	2.41 ± 0.05	$2.424\ 5$
Blind via		
Height	1.07 ± 0.03	$1.052\ 376$
Laminate thickness		
Gore	0.078 ± 0.003	$0.077\ 831$
Rogers 4003	0.92 ± 0.03	$0.894\ 081$
SRR dimensions		
Via-via distance	2.51 ± 0.02	$2.512\ 1047$
Gap	0.320 ± 0.006	$0.319\ 7473$
Outer layer, thickness	0.094 ± 0.009	$0.093\ 967$
Outer layers, width	0.176 ± 0.009	$0.176\ 1885$
Outer layers, length	2.90 ± 0.06	$2.899\ 336$
Wire dimensions		
Thickness	0.0249 ± 0.0004	$0.0249\ 06$
Width	0.500 ± 0.005	0.50

boards. Both of the Rogers circuit boards initially have a thin layer of copper (half-ounce, or ~12 μm in thickness) deposited on both sides from which the elements are patterned using conventional optical lithography. The wire elements are patterned on the sides of the Rogers boards that face the Gore SpeedBoard, as shown in Fig. 1. The particular dual wire geometry used was chosen so that the structure would maintain reflection symmetry in the direction of wave propagation. Symmetric structures are convenient when performing the retrieval of the material parameters from the scattering (S-) parameters, described below. A single wire placed in the center of the structure would give nearly identical results, but such a placement is not possible in the current multilayer design.

Two sides of the nominally rectangular SRR element are patterned on the outside faces of the Rogers circuit board. The remaining two perpendicular sides are formed from vias—plated through holes—that extend through laminate layers of the circuit board. One side is formed by a through via extending continuously through all three layers of circuit board. The last side of the SRR is formed by two blind vias, terminating at either side of the center laminate layer. Small annular rings introduce the capacitive gap. A side view of the resulting SRR is shown in Fig. 2.

Using the driven solution in (HFSS) (Ansoft), a finite-element based software package that solves Maxwell's equations, the S-parameters were simulated for variations of the unit cell shown in Fig. 1, and the material parameters retrieved by standard methods.[8] Through this analysis, a suitable structure was found that provided a nearly matched negative index band over x-band frequencies. The optimized structure was then fabricated by a commercial vendor (Hughes Circuits, San Marcos, CA). Before performing scattering measurements on the sample, detailed physical measurements were performed so that the best comparison with numerical simulations could be obtained. Several cuts in different planes were made in one of the sample sheets. Each of the resulting faces was then polished and photographed under a microscope. The dimensions of each of the critical elements in the structure were determined by counting pixels in the corresponding digital image. Calibration was achieved using a hardness test divot whose length was known to 0.1 μm. The physical measurements, summarized in Table I, were then used in the comparison simulations shown below.

To experimentally confirm the expected properties of the negative index composite, the magnitude and phase of the S-parameters (S_{11} and S_{21}) were measured. The experiments were performed in free space using an apparatus similar to that previously reported.[9] In the experiment, an Agilent 8510B vector network analyzer was used to sweep microwaves over a frequency range 7–13 GHz. Two microwave horns (Rozendal Associates Inc., Santee, CA) were used as the source and detector. Lens assemblies mounted on the horns produced a focused spot at a distance of approximately 30.5 cm (12 in.). The sample was placed at the focus. For transmission experiments, a confocal setup was used, in which both the source and detector horns were placed one focal length from the sample. Calibration was performed using a "through" measurement, in which the transmitted power was measured in the absence of any material. For the
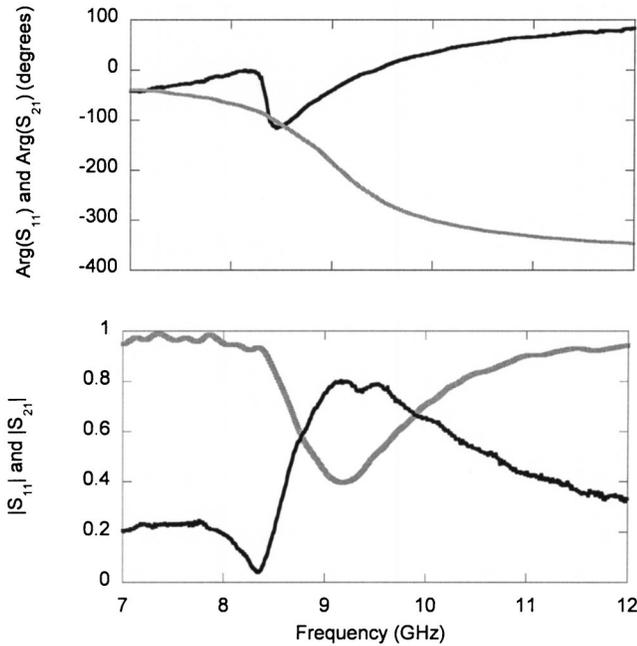
FIG. 3. *S*-parameters for a single layer of the negative index composite. (a) Phase of S_{21} (black curve) and S_{11} (gray curve). (b) Magnitude of S_{21} (black curve) and S_{11} (gray curve).

reflection measurement, the horns were moved to the same side of the sample. Because of the finite size of the horn/lens assemblies, the two horns were offset from each other such that the power was incident at an angle of $\sim 16°$ from the surface normal of the sample. The reflection was calibrated by measuring the reflected power from an aluminum plate— assumed a perfect reflector (with a 180° phase shift) for this measurement.

The magnitude and phase of the *S*-parameters for a single layer of the negative index composite are presented in Fig. 3. A method of demonstrating negative index in past work has been to first measure the transmitted power through a sample of SRRs alone, identifying the frequency range of the stop band where $\mu < 0$; then measure the power transmitted through a wire structure alone; and finally measure the power transmitted through the composite structure. This method is convenient when phase data is not available and when the frequency of negative index forms a well-defined pass band. As can be seen from Fig. 3, however, there are no readily identifiable features from the single layer transmitted power [Fig. 3(b)] that clearly indicate negative index. However, the noise level of the measured phase data [Fig. 3(a)] is quite low, implying that the full *S*-parameters retrieval procedure should provide stable results.

The full retrieval of the material parameters for a metamaterial proceeds by a measurement of the transmitted and reflected amplitudes and phases from a slab of finite thickness. For continuous, isotropic materials, the transmission and reflection coefficients have analytic forms that can be readily inverted.[8] For example, the inversion of the scattering equations leads to the following form that allows determination of the refractive index:

$$\cos(nkd) = \text{Re}\left(\frac{1}{S_{21}}\right) - \frac{1}{2|S_{21}|^2}(A_1 S_{11} + A_2 S_{21}), \quad (1)$$

where A_1 and A_2 are real valued functions that tend to zero in the absence of losses. Equation (1) shows that, for a lossless sample, the index can be determined from just the phase and amplitude of S_{21}. Furthermore, for roughly matched samples, Eq. (1) indicates a strong correlation between the phase of S_{21} and the index. The dip in the phase of S_{21}, shown in Fig. 3(a), is thus an indicator that our sample possesses a negative refractive index somewhere over the frequency region between 8–9 GHz. Having all components available from our measurements however, we need not rely on this approximation but can recover exact functions for the complex index, as well as the complex impedance, which is given by the following:[8]

$$z = \pm \sqrt{\frac{(1 + S_{11})^2 - S_{21}^2}{(1 - S_{11})^2 - S_{21}^2}}. \quad (2)$$

A retrieval procedure to determine the impedance (z) and the index (n) was carried out on both the measured *S*-parameter data as well as the *S*-parameters simulated in HFSS. Although the retrieval of n is generally complicated by multiple branches due to the arccosine function in Eq. (1), the branches are sufficiently separated for the thin sample measured (one unit cell in thickness) that no sophisticated retrieval algorithm was necessary. There is, however, a sign ambiguity in n and z that can be eliminated by imposing that $\text{Re}(z) > 0$ and $\text{Im}(n) > 0$—requirements necessary for a causal material. No other manipulation was performed on the data, other than to apply a 31 point smoothing on the measured *S*-parameter data to reduce the impact of voltage standing-wave ratio (VSWR) resonances inherent to the setup. Note that Eqs. (1) and (2) neglect any possible effects due to chirality or bianisotropy. Our negative index composite was designed so as to eliminate or at least minimize any magnetodielectric coupling, so that these simple formulas would be approximately valid for the retrieval procedure.[10]

The retrieved z and n are shown in Figs. 4(a) and 4(b), respectively. A negative index frequency band occurs in the measured sample between 8.4 and 9.2 GHz. The agreement between the simulated and measured data over the negative index region is excellent, both quantitatively and qualitatively. Any existing disagreement between the four sets of curves could be further minimized by making slight alterations to the material parameters, for example, adjusting the conductivity used for the copper elements. Some of the disagreement might be caused by the non-normal incidence used in the S_{11} measurement.

The permittivity (ε) and the permeability (μ) are simply related to n and z according to $\varepsilon = n/z$ and $\mu = nz$. The retrieved frequency dependent ε and μ are presented in Fig. 5, having been obtained from the values of n and z plotted in Fig. 4. As is consistent with previous theoretically obtained results, the real part of ε exhibits a zero, below which it is negative. Also, μ of the composite exhibits a characteristic resonant form, due primarily to the response of the SRRs, that has a region where the real part of μ is negative. The
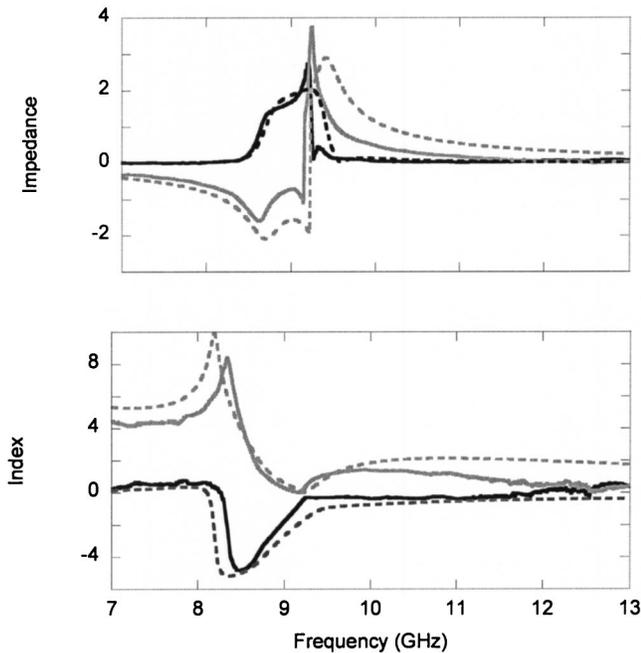
FIG. 4. (a) Recovered impedance (z) from simulation data (dashed curves) and from measured S-parameters (solid curves) for one unit cell of the structure. (b) Recovered refractive index (n) from simulation data (dashed curves) and from measured S-parameters (solid curves). Black curves are the real parts, gray curves are the imaginary parts.

FIG. 5. (a) Recovered permittivity (ε) from simulation data (dashed curves) and from measurement data (solid curves) for one unit cell of the structure. (b) Recovered permeability (μ) from simulation data (dashed curves) and from measurement data (solid curves). Black curves are the real parts, gray curves are the imaginary parts.

frequency band where both real parts of ε and μ are negative is consistent with the negative index band found in Fig. 4(b).

In summary, we have presented a composite metamaterial that possesses a frequency band over which the refractive index is negative. The structure has advantages in terms of fabrication, being entirely assembled using conventional multilayer circuit board technology that obviates the need for cutting and further assembly steps. While the structure is somewhat more complicated in design than earlier materials, it is amenable to numerical simulations which show excellent agreement with the measured structures.

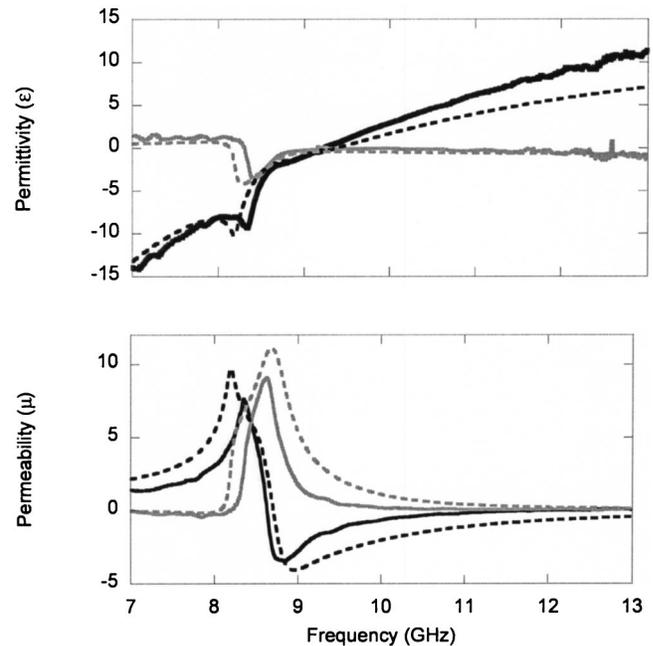In our characterization, we have shown that a full

S-parameters retrieval provides complete information on the material parameters of the sample in a direct manner. While indirect methods, such as Snell's law measurements, can provide important complementary information, the S-parameters measurement and retrieval can form the basis of a semi-automated metamaterial characterization procedure.

---

*Also at SensorMetrix, 5965 Pacific Center Blvd., Ste. 701, San Diego, CA 92121-4323.

†Also at Department of Physics, University of California, San Diego, La Jolla, CA 92093.

[1] V. G. Veselago, Sov. Phys. Usp. **10**, 509 (1968).

[2] J. B. Pendry, A. J. Holden, W. J. Stewart, and I. Youngs, Phys. Rev. Lett. **76**, 4773 (1996).

[3] J. B. Pendry, A. J. Holden, D. J. Robbins, and W. J. Stewart, IEEE Trans. Microwave Theory Tech. **47**, 2075 (1999).

[4] D. R. Smith, W. Padilla, D. C. Vier, S. C. Nemat-Nasser, and S. Schultz, Phys. Rev. Lett. **84**, 4184 (2000).

[5] R. A. Shelby, D. R. Smith, and S. Schultz, Science **292**, 79 (2001).

[6] C. G. Parazzoli, R. B. Greegor, K. Li, B. E. C. Koltenbah, and M. Tanielian, Phys. Rev. Lett. **90**, 107401 (2003).

[7] A. A. Houck, J. B. Brock, and I. L. Chuang, Phys. Rev. Lett. **90**, 137401 (2003).

[8] D. R. Smith, S. Schultz, P. Markos, and C. M. Soukoulis, Phys. Rev. B **65**, 195104 (2002).

[9] R. B. Greegor, C. G. Parazzoli, K. Li, B. E. C. Koltenbah, and M. Tanielian, Opt. Express **11**, 688 (2003).

[10] R. Marques, F. Medina, and R. Rafii-El-Idrissi, Phys. Rev. B **65**, 144440 (2002).